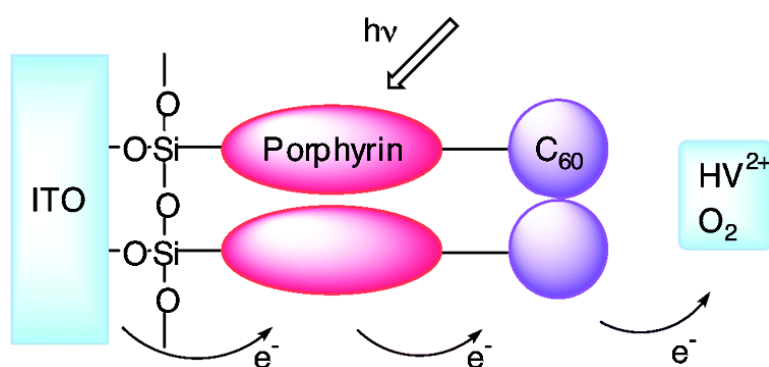Article

Photovoltaic Properties of Self-Assembled Monolayers of Porphyrins and Porphyrin–Fullerene Dyads on ITO and Gold Surfaces

Hiroko Yamada, Hiroshi Imahori, Yoshinobu Nishimura, Iwao Yamazaki,
Tae Kyu Ahn, Seong Keun Kim, Dongho Kim, and Shunichi Fukuzumi

More About This Article

Additional resources and features associated with this article are available within the HTML version:

- Supporting Information
- Links to the 27 articles that cite this article, as of the time of this article download
- Access to high resolution figures
- Links to articles and content related to this article
- Copyright permission to reproduce figures and/or text from this article

View the Full Text HTML

Photovoltaic Properties of Self-Assembled Monolayers of Porphyrins and Porphyrin−Fullerene Dyads on ITO and Gold Surfaces

Hiroko Yamada,[†] Hiroshi Imahori,*,[‡] Yoshinobu Nishimura,[§] Iwao Yamazaki,*,[§]
Tae Kyu Ahn,[‖,⊥] Seong Keun Kim,[⊥] Dongho Kim,*,[‖] and Shunichi Fukuzumi*,[†]

*Contribution from the Department of Material and Life Science, Graduate School of
Engineering, Osaka University, CREST, Japan Science and Technology Corporation (JST),
Suita, Osaka 565-0871, Japan, Department of Molecular Engineering, Graduate School of
Engineering, Kyoto University, PRESTO, Japan Science and Technology Corporation (JST),
Kyoto 615-8510, Japan, Fukui Institute for Fundamental Chemistry, Kyoto University,
34-4, Takano-Nishihiraki-cho, Sakyo-ku, Kyoto 606-8103, Japan, Department of Molecular
Chemistry, Graduate School of Engineering, Hokkaido University, Sapporo 060-8628, Japan,
the Center for Ultrafast Optical Characteristics Control, Department of Chemistry,
Yonsei University, Seoul 120-749, Korea, and School of Chemistry, Seoul National University,
Seoul 151-747, Korea*

Received February 28, 2003; E-mail: imahori@scl.kyoto-u.ac.jp; yamiw@eng.hokudai.ac.jp;
dongho@yonsei.ac.kr; fukuzumi@ap.chem.eng.osaka-u.ac.jp

Abstract: A systematic series of ITO electrodes modified chemically with self-assembled monolayers (SAMs) of porphyrins and porphyrin−fullerene dyads have been designed to provide valuable insight into the development of artificial photosynthetic devices. First the ITO and gold electrodes modified chemically with SAMs of porphyrins with a spacer of the same number of atoms were prepared to compare the effects of energy transfer (EN) quenching of the porphyrin excited singlet states by the two electrodes. Less EN quenching was observed on the ITO electrode as compared to the EN quenching on the corresponding gold electrode, leading to remarkable enhancement of the photocurrent generation (ca. 280 times) in the porphyrin SAMs on the ITO electrode in the presence of the triethanolamine (TEA) used as a sacrificial electron donor. The porphyrin (H_2P) was then linked with C_{60} which can act as an electron acceptor to construct H_2P-C_{60} SAMs on the ITO surface in the presence of hexyl viologen (HV^{2+}) used as an electron carrier in a three electrode system, denoted as ITO/H_2P-C_{60}/HV^{2+}/Pt. The quantum yield of the photocurrent generation of the ITO/H_2P-C_{60}/HV^{2+}/Pt system (6.4%) is 30 times larger than that of the corresponding system without C_{60}: ITO/H_2P-ref/HV^{2+}/Pt (0.21%). Such enhancement of photocurrent generation in the porphyrin−fullerene dyad system is ascribed to an efficient photoinduced ET from the porphyrin singlet excited state to the C_{60} moiety as indicated by the fluorescence lifetime measurements and also by time-resolved transient absorption studies on the ITO systems. The surface structures of H_2P and H_2P-C_{60} SAMs on ITO (H_2P/ITO and H_2P-C_{60}/ITO) have been observed successfully in molecular resolution with atomic force microscopy for the first time.

Introduction

Molecular engineering of artificial self-assemblies at surfaces with desired functions has recently attracted much interest as advancement of nanotechnology. Self-assembled monolayers (SAMs) are highly promising to construct such molecular architectures on metal and semiconductor surfaces.[1] In this context, alkanethiols on gold surfaces are the most well-studied systems which provide densely packed, well-ordered structures on the surface.[1] Thus, functionalization on the surfaces has been achieved by incorporating potential chromophores such as fullerenes,[2−4] porphyrins,[5−8] and others[9,10] at the end of alkanethiols

or equivalents. However, the performance of SAMs as molecular devices is extremely sensitive to the structures and properties of functionalized SAMs, which have been difficult to control.

SAMs of photoactive chromophores on the flat gold surface[4,5,8,10−12] have merited special attention as artificial

† Osaka University.
‡ Kyoto University.
§ Hokkaido University.
‖ Yonsei University.
⊥ Seoul National University.

(1) (a) Ulman, A. *An Introduction to Ultrathin Organic Films*; Academic Press: San Diego, 1991. (b) *Molecular Electronics*; Jortner, J., Ratner, M. Eds.; Blackwell Science: Oxford, 1997. (c) Mirkin, C. A. *Inorg. Chem.* **2000**, *39*, 2258. (d) Shipway, A. N.; Katz, E.; Willner, I. *ChemPhysChem* **2000**, *1*, 18. (e) Alivisatos, A. P.; Barbara, P. F.; Castleman, A. W.; Chang, J.; Dixon, D. A.; Klein, M. L.; McLendon, G. L.; Miller, J. S.; Ratner, M. A.; Rossky, P. J.; Stupp, S. I.; Thompson, M. E. *Adv. Mater.* **1998**, *10*, 1297.
(2) (a) Mirkin, C. A.; Caldwell, W. B. *Tetrahedron* **1996**, *52*, 5113. (b) Shi, X.; Caldwell, W. B.; Chen, K.; Mirkin, C. A. *J. Am. Chem. Soc.* **1994**, *116*, 11598. (c) Caldwell, W. B.; Chen, K.; Mirkin, C. A.; Babinec, S. J. *Langmuir* **1993**, *9*, 1945. (d) Shon, Y.-S.; Kelly, K. F.; Halas, N. J.; Lee, T. R. *Langmuir* **1999**, *15*, 5329. (e) Hatano, T.; Ikeda, A.; Akiyama, T.; Yamada, S.; Sano, M.; Kanekiyo, Y.; Shinkai, S. *J. Chem. Soc., Perkin Trans. 2* **2000**, *5*, 909.

photosynthetic materials and photonic molecular devices. In particular, donor−acceptor linked molecules[5,13] or donor−acceptor mixed components[14] have been employed in such systems to mimic photosynthetic electron transfer (ET) and energy transfer (EN) on the gold electrode. However, strong EN quenching of the excited states of chromophores by the gold surface has precluded achievement of a high quantum yield for charge separation (CS) on the surface as attained in photosyn-

thesis. To surmount such an EN quenching problem, indium−tin oxide (ITO) with high optical transparency (>90%) and electrical conductivity (∼10 Ω cm) seems to be the most promising candidate as an electrode which may suppress the quenching of the excited states of adsorbed dyes on the surface. Despite these advantages, development of SAMs on the ITO electrode has been limited in that their chemical modification requires carefully controlled conditions which have been difficult to achieve.[15] Only a single chromophore has so far been attached on the ITO electrode.[16−21] Thus, SAMs of donor−acceptor linked molecules on ITO have yet to be constructed to compare the EN quenching of chromophores by the ITO electrode and by the corresponding gold electrode.

Fullerenes have frequently been used as an acceptor in donor−acceptor linked molecules.[22,23] Fullerenes have small reorganization energies of ET, which lead to remarkable acceleration of photoinduced CS and of charge shift (CSH) and retardation of charge recombination (CR) in donor-fullerene linked molecules.[23−25] Since porphyrins used as donors as well

(3) (a) Arias, F.; Godínez, L. A.; Wilson, S. R.; Kaifer, A. E.; Echegoyen, L. *J. Am. Chem. Soc.* **1996**, *118*, 6086. (b) Domínguez, O.; Echegoyen, L.; Cunha, F.; Tao, N. *Langmuir* **1998**, *14*, 821. (c) Echegoyen, L.; Echegoyen, L. E. *Acc. Chem. Res.* **1998**, *31*, 593. (d) Liu, S.-G.; Martineau, C.; Raimundo, J.-M.; Roncali, J.; Echegoyen, L. *Chem. Commun.* **2001**, 913.

(4) Imahori, H.; Azuma, T.; Ajavakom, A.; Norieda, H.; Yamada, H.; Sakata, Y. *J. Phys. Chem. B* **1999**, *103*, 7233.

(5) (a) Lahav, M.; Gabriel, T.; Shipway, A. N.; Willner, I. *J. Am. Chem. Soc.* **1999**, *121*, 258. (b) Lahav, M.; Heleg-Shabtai, V.; Wasserman, J.; Katz, E.; Willner, I.; Dürr, H.; Hu, Y.-Z.; Bossmann, S. H. *J. Am. Chem. Soc.* **2000**, *122*, 11480. (c) Uosaki, K.; Kondo, T.; Zhang, X.-Q.; Yanagida, M. *J. Am. Chem. Soc.* **1997**, *119*, 8367. (d) Kondo, T.; Yanagida, M.; Nomura, S.-i.; Ito, T.; Uosaki, K. *J. Electroanal. Chem.* **1997**, *438*, 121. (e) Abdelrazzaq, F. B.; Kwong, R. C.; Thompson, M. E. *J. Am. Chem. Soc.* **2002**, *124*, 4796.

(6) (a) Katz, E.; Willner, I. *Langmuir* **1997**, *13*, 3364. (b) Zak, J.; Yuan, H.; Ho, M.; Woo, L. K.; Porter, M. D. *Langmuir* **1993**, *9*, 2772. (c) Hutchison, J. E.; Postlethwaite, T. A.; Chen, C.-h.; Hathcock, K. W.; Ingram, R. S.; Ou, W.; Linton, R. W.; Murray, R. W.; Tyvoll, T. A.; Chng, L. L.; Collman, J. P. *Langmuir* **1997**, *13*, 2143. (d) Hutchison, J. E.; Postlethwaite, T. A.; Murray, R. W. *Langmuir* **1993**, *9*, 3277. (e) Simpson, T. R. E.; Revell, D. J.; Cook, M. J.; Russell, D. A. *Langmuir* **1997**, *13*, 460. (f) Gryko, D. T.; Zhao, F.; Yasseri, A. A.; Roth, K. M.; Bocian, D. F.; Kuhr, W. G.; Lindsey, J. S. *J. Org. Chem.* **2000**, *65*, 7356.

(7) (a) Ashkenasy, G.; Kalyuzhny, G.; Libman, J.; Rubinstein, I.; Shanzer, A. *Angew. Chem., Int. Ed.* **1999**, *38*, 1257. (b) Kanayama, N.; Kanbara, T.; Kitano, H. *J. Phys. Chem. B* **2000**, *104*, 271. (c) Offord, D. A.; Sachs, S. B.; Ennis, M. S.; Eberspacher, T. A.; Griffin, J. H.; Chidsey, C. E. D.; Collman, J. P. *J. Am. Chem. Soc.* **1998**, *120*, 4478. (d) Willner, I.; Heleg-Shabtai, V.; Katz, E.; Rau, H. K.; Haehnel, W. *J. Am. Chem. Soc.* **1999**, *121*, 6455.

(8) (a) Fukuzumi, S.; Imahori, H. In *Electron Transfer in Chemistry*; Balzani, V., Ed.; Wiley-VCH: Weinheim, 2001; Vol. 2, pp 927−975. (b) Imahori, H.; Norieda, H.; Ozawa, S.; Ushida, K.; Yamada, H.; Azuma, T.; Tamaki, K.; Sakata, Y. *Langmuir* **1998**, *14*, 5335. (c) Imahori, H.; Norieda, H.; Nishimura, Y.; Yamazaki, I.; Higuchi, K.; Kato, N.; Motohiro, T.; Yamada, H.; Tamaki, K.; Arimura, M.; Sakata, Y. *J. Phys. Chem. B* **2000**, *104*, 1253.

(9) (a) Hickman, J. J.; Ofer, D.; Zou, C.; Wrighton, M. S.; Laibinis, P. E.; Whitesides, G. M. *J. Am. Chem. Soc.* **1991**, *113*, 1128. (b) Frisbie, C. D.; Martin, J. R.; Duff, R. R., Jr.; Wrighton, M. S. *J. Am. Chem. Soc.* **1992**, *114*, 7142. (c) Creager, S.; Yu, C. J.; Bamdad, C.; O'Connor, S.; MacLean, T.; Lam, E.; Chong, Y.; Olsen, G. T.; Luo, J.; Gozin, M.; Kayyem, J. F. *J. Am. Chem. Soc.* **1999**, *121*, 1059. (d) Kondo, T.; Horiuchi, S.; Yagi, I.; Ye, S.; Uosaki, K. *J. Am. Chem. Soc.* **1999**, *121*, 391. (e) Byrd, H.; Suponeva, E. P.; Bocarsly, A. B.; Thompson, M. E. *Nature* **1996**, *380*, 610.

(10) (a) Caldwell, W. B.; Campbell, D. J.; Chen, K.; Herr, B. R.; Mirkin, C. A.; Malik, A.; Durbin, M. K.; Dutta, P.; Huang, K. G. *J. Am. Chem. Soc.* **1995**, *117*, 6071. (b) Campbell, D. J.; Herr, B. R.; Hulteen, J. C.; Van Duyne, R. P.; Mirkin, C. A. *J. Am. Chem. Soc.* **1996**, *118*, 10211. (c) Walter, D. G.; Campbell, D. J.; Mirkin, C. A. *J. Phys. Chem. B* **1999**, *103*, 402.

(11) (a) Willner, I. *Acc. Chem. Res.* **1997**, *30*, 347. (b) Blonder, E.; Levi, S.; Tao, G.; Ben-Dov, I.; Willner, I. *J. Am. Chem. Soc.* **1997**, *119*, 10467. (c) Doron, A.; Portnoy, M.; Lion-Dagan, M.; Katz, E.; Willner, I. *J. Am. Chem. Soc.* **1996**, *118*, 8937. (d) Morita, T.; Kimura, S.; Kobayashi, S.; Imanishi, Y. *J. Am. Chem. Soc.* **2000**, *122*, 2850. (e) Roth, K. M.; Lindsey, J. S.; Bocian, D. F.; Kuhr, W. G. *Langmuir* **2002**, *18*, 4030.

(12) (a) Fox, M. A. *Acc. Chem. Res.* **1999**, *32*, 201. (b) Wolf, M. O.; Fox, M. A. *J. Am. Chem. Soc.* **1995**, *117*, 1845. (c) Wolf, M. O.; Fox, M. A. *Langmuir* **1996**, *12*, 955. (d) Fox, M. A.; Wooten, M. D. *Langmuir* **1997**, *13*, 7099. (e) Li, W.; Lynch, V.; Thompson, H.; Fox, M. A. *J. Am. Chem. Soc.* **1997**, *119*, 7211. (f) Reese, S.; Fox, M. A. *J. Phys. Chem. B* **1998**, *102*, 9820.

(13) (a) Akiyama, T.; Imahori, H.; Ajavakom, A.; Sakata, Y. *Chem. Lett.* **1996**, 907. (b) Imahori, H.; Ozawa, S.; Ushida, K.; Takahashi, M.; Azuma, T.; Ajavakom, A.; Akiyama, T.; Hasegawa, M.; Taniguchi, S.; Okada, T.; Sakata, Y. *Bull. Chem. Soc. Jpn.* **1999**, *72*, 485. (c) Imahori, H.; Yamada, H.; Ozawa, S.; Ushida, K.; Sakata, Y. *Chem. Commun.* **1999**, 1165. (d) Imahori, H.; Yamada, H.; Nishimura, Y.; Yamazaki, I.; Sakata, Y. *J. Phys. Chem. B* **2000**, *104*, 2099. (e) Imahori, H.; Norieda, H.; Yamada, H.; Nishimura, Y.; Yamazaki, I.; Sakata, Y.; Fukuzumi, S. *J. Am. Chem. Soc.* **2001**, *123*, 100. (f) Hirayama, D.; Yamashiro, T.; Takimiya, K.; Aso, Y.; Otsubo, T.; Norieda, H.; Imahori, H.; Sakata, Y. *Chem. Lett.* **2000**, 570.

(14) (a) Imahori, H.; Nishimura, Y.; Norieda, H.; Karita, H.; Yamazaki, I.; Sakata, Y.; Fukuzumi, S. *Chem. Commun.* **2000**, 661. (b) Imahori, H.; Hasobe, T.; Yamada, H.; Nishimura, Y.; Yamazaki, I.; Fukuzumi, S. *Langmuir* **2001**, *17*, 4925. (c) Morita, T.; Kimura, S.; Kobayashi, S.; Imanishi, Y. *Chem. Lett.* **2000**, 676. (d) Imahori, H.; Fukuzumi, S. *Adv. Mater.* **2001**, *13*, 1197.

(15) (a) Suto, S.; Uchida, W.; Yashima, M.; Goto, T. *Phys. Rev. B* **1987**, *35*, 4393. (b) Choudhury, B.; Weedon, A. C.; Bolton, J. R. *Langmuir* **1998**, *14*, 6199. (c) *Molecular Design of Electrode Surfaces*; Murray, R. W., Ed.; John Wiley & Sons: New York, 1992; pp 1−48.

(16) (a) Eckert, J.-F.; Nicoud, J.-F.; Nierengarten, J.-F.; Liu, S.-G.; Echegoyen, L.; Barigelletti, F.; Armaroli, N.; Ouali, L.; Krasnikov, V.; Hadziioannou, G. *J. Am. Chem. Soc.* **2000**, *122*, 7467. (b) Gu, T.; Tsamouras, D.; Melzer, C.; Krasnikov, V.; Gisselbrecht, J. P.; Gross, M.; Hadziioannou, G.; Nierengarten, J. O. *ChemPhysChem* **2002**, *3*, 124. (c) Nierengarten, J.-F.; Eckert, J.-F.; Nicoud, J.-F.; Ouali, L.; Krasnikov, V.; Hadziioannou, G. *Chem. Commun.* **1999**, 617. (d) Peeters, E.; van Hal, P. A.; Knol, J.; Brabec, C. J.; Sariciftci, N. S.; Hummelen, J. C.; Janssen, R. A. J. *J. Phys. Chem. B* **2000**, *104*, 10174.

(17) (a) Obeng, Y. S.; Bard, A. J. *Langmuir* **1991**, *7*, 195. (b) Chen, K.; Caldwell, W. B.; Mirkin, C. A. *J. Am. Chem. Soc.* **1993**, *115*, 1193. (c) Ikeda, A.; Hatano, T.; Shinkai, S.; Akiyama, T.; Yamada, S. *J. Am. Chem. Soc.* **2001**, *123*, 4855. (d) Wei, T.-X.; Zhai, J.; Ge, J.-H.; Gan, L.-B.; Huang, C.-H.; Luo, G.-B.; Ying, L.-M.; Liu, T.-T.; Zhao, X.-S. *Appl. Surf. Sci.* **1999**, *151*, 153. (e) Hasobe, T.; Imahori, H.; Yamada, H.; Sato, T.; Ohkubo, K.; Fukuzumi, S. *Nano Lett.* **2003**, *3*, 409.

(18) SAMs of photoactive single chromophores on other metal oxides (i.e., SnO₂ and TiO₂) have revealed photocurrent generation; see: (a) Osa, T.; Fujihira, M. *Nature* **1976**, *264*, 349. (b) Fujihira, M.; Ohishi, N.; Osa, T. *Nature* **1977**, *268*, 226. (c) Anderson, S.; Constable, E. C.; Dare-Edwards, M. P.; Goodenough, J. B.; Hamnett, A.; Seddon, K. R.; Wright, R. D. *Nature* **1979**, *280*, 571. (d) Fox, M. A.; Nobes, F. J.; Voynick, T. A. *J. Am. Chem. Soc.* **1980**, *102*, 4036. (e) Hagfeldt, A.; Grätzel, M. *Acc. Chem. Res.* **2000**, *33*, 269.

(19) SAMs of donor−acceptor dyad systems on nanoparticulate semiconductors (i.e., TiO₂) have been reported to generate photocurrent; see: (a) Argazzi, R.; Bignozzi, C. A.; Heimer, T. A.; Castellano, F. N.; Meyer, G. J. *J. Am. Chem. Soc.* **1995**, *117*, 11815. (b) Bonhôte, P.; Moser, J.-E.; Humphry-Baker, R.; Vlachopoulos, N.; Zakeeruddin, S. M.; Walder, L.; Grätzel, M. *J. Am. Chem. Soc.* **1999**, *121*, 1324. (c) Kleverlaan, C. J.; Indelli, M. T.; Bignozzi, C. A.; Pavanin, L.; Scandola, F.; Hasselman, G. M.; Meyer, G. J. *J. Am. Chem. Soc.* **2000**, *122*, 2840. (d) Kamat, P. V.; Barazzouk, S.; Hotchandani, S.; Thomas, K. G. *Chem.—Eur. J.* **2000**, *6*, 3914.

(20) Vectorial photoinduced ET of chlorin-C₆₀ dyad incorporated noncovalently into Langmuir−Blodgett (LB) films on ITO was confirmed by time-resolved Maxwell displacement charge measurements; see: (a) Tkachenko, N. V.; Vuorimaa, E.; Kesti, T.; Alekseev, A. S.; Tauber, A. Y. Hynninen, P. H.; Lemmetyinen, H. *J. Phys. Chem. B* **2000**, *104*, 6371. (b) Tkachenko, N. V.; Vehmanen, V.; Nikkanen, J.-P.; Yamada, H.; Imahori, H.; Fukuzumi, S.; Lemmetyinen, H. *Chem. Phys. Lett.* **2002**, *366*, 245.

(21) Layer-by-layer noncovalent deposition of ruthenium complex-C₆₀ dyad on ITO was reported for the fabrication of photoactive films exhibiting photocurrent generation; see: Luo, C.; Guldi, D. M.; Maggini, M.; Menna, E.; Mondini, S.; Kotov, N. A.; Prato, M. *Angew. Chem., Int. Ed.* **2000**, *39*, 3905.

(22) (a) Martín, N.; Sánchez, L.; Illescas, B.; Pérez, I. *Chem. Rev.* **1998**, *98*, 2527. (b) Prato, M. *J. Mater. Chem.* **1997**, *7*, 1097. (c) Diederich, F.; Gómez-López, M. *Chem. Soc. Rev.* **1999**, *28*, 263. (d) Guldi, D. M.; Kamat, P. V. In *Fullerenes*; Kadish, K. M., Ruoff, R. S., Eds.; John Wiley & Sons: New York, 2000; Chapter 5, pp 225−281. (e) Gust, D.; Moore, T. A.; Moore, A. L. *Acc. Chem. Res.* **2001**, *34*, 40. (f) Jensen, A. W.; Wilson, S. R.; Schuster, D. I. *Bioorg. Med. Chem.* **1996**, *4*, 767. (g) Verhoeven, J. W. *Adv. Chem. Phys.* **1999**, *106*, 603.

(23) (a) Imahori, H.; Sakata, Y. *Adv. Mater.* **1997**, *9*, 537. (b) Imahori, H.; Sakata, Y. *Eur. J. Org. Chem.* **1999**, *2445*, 5. (c) Guldi, D. M. *Chem. Commun.* **2000**, 321. (d) Guldi, D. M.; Prato, M. *Acc. Chem. Res.* **2000**, *33*, 695. (e) Imahori, H.; Mori, Y.; Matano, Y. *J. Photochem. Photobiol., C* **2003**, *4*, 51.
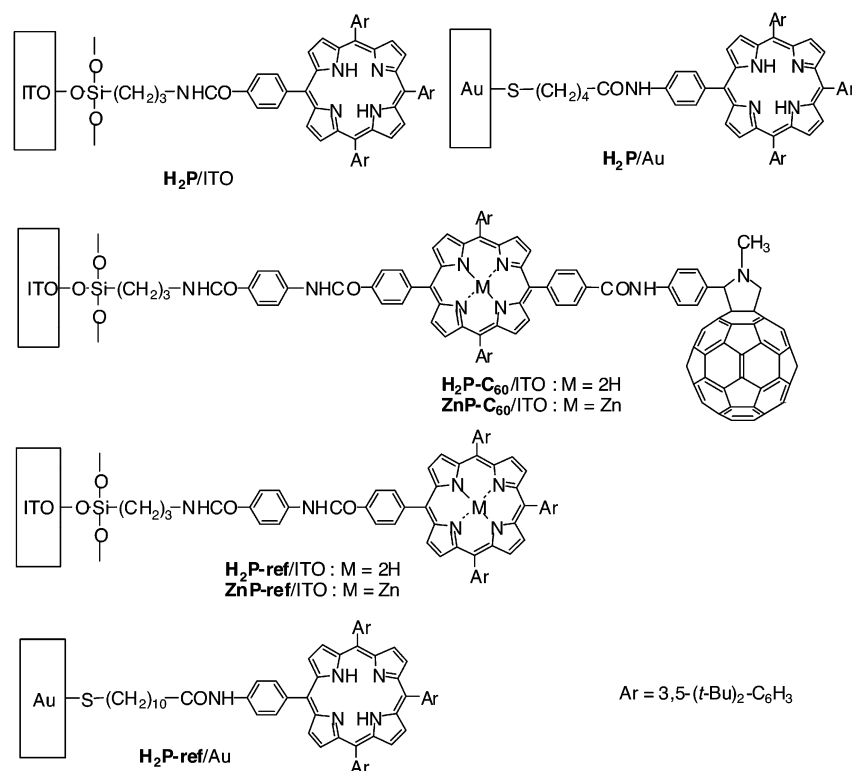
Figure 1. Self-assembled monolayers of porphyrins and porphyrin−fullerene dyads on ITO and gold electrodes.

as sensitizers are also known to exhibit small reorganization energies of ET,[23,24] a combination of both chromophores (i.e., porphyrins and fullerenes) is ideal to generate a long-lived charge-separated state with a high quantum yield on electrodes[13] as well as in solutions.[23,24]

We report herein construction of SAMs of porphyrin−fullerene dyads on the ITO electrode and the reference SAMs on the gold electrode to compare the EN quenching of the porphyrin chromophore by the ITO electrode and by the corresponding gold electrode. The investigated systems are shown in Figure 1. The extensive SAM series are porphyrin SAMs on the ITO electrode (denoted as **H₂P**/ITO),[26] those on the gold electrode with a spacer of the same number of atoms (denoted as **H₂P**/Au),[8c] SAMs of porphyrin (P)−C₆₀ linked molecules on the ITO electrode [denoted as **P-C₆₀**/ITO (P=H₂P or ZnP)],[27] the corresponding reference SAMs without C₆₀ with the same spacer on the ITO electrode (denoted as **P-ref**/ITO), and the reference porphyrin SAMs on the gold

electrode with a spacer of the same number of atoms[8c] (denoted as **H₂P-ref**/Au). The photovoltaic properties of the SAM series in Figure 1 are examined by photoelectrochemical measurements together with fluorescence lifetime measurements and also by time-resolved transient absorption studies on the ITO systems. The surface structures of **H₂P** and **H₂P-C₆₀** SAMs on ITO (**H₂P**/ITO and **H₂P-C₆₀**/ITO) are also clarified in molecular resolution using atomic force microscopy. Thus, the present study provides valuable data for realization of molecular-level photovoltaic devices in which efficient multistep electron transfer occurs on the electrodes as attained in photosynthesis.

Results and Discussion

Synthesis. The general strategy employed for synthesizing the SAMs is summarized in the Supporting Information (see Supporting Information S7 and S8). Porphyrin SAMs on gold electrodes (**H₂P**/Au and **H₂P-ref**/Au) were obtained by following the same procedures as described previously.[8c] Porphyrin references (**H₂P-ref**, **ZnP-ref**,[28] and **H₂P**[29]) and porphyrin−fullerene dyads (**H₂P-C₆₀** and **ZnP-C₆₀**)[30] were also synthesized (Figure 2). Structures of all new compounds were confirmed by spectroscopic analysis including ¹H NMR and FAB mass spectra (see the Supporting Information).

Porphyrin SAMs on ITO and Gold Electrodes. Figure 3 displays absorption spectra of **H₂P**/ITO and porphyrin reference

(24) (a) Imahori, H.; Hagiwara, K.; Akiyama, T.; Aoki, M.; Taniguchi, S.; Okada, T.; Shirakawa, M.; Sakata, Y. *Chem. Phys. Lett.* **1996**, *263*, 545. (b) Tkachenko, N. V.; Guenther, C.; Imahori, H.; Tamaki, K.; Sakata, Y.; Fukuzumi, S.; Lemmetyinen, H. *Chem. Phys. Lett.* **2000**, *326*, 344. (c) Imahori, H.; Tamaki, K.; Yamada, H.; Yamada, K.; Sakata, Y.; Nishimura, Y.; Yamazaki, I.; Fujitsuka, M.; Ito, O. *Carbon* **2000**, *38*, 1599. (d) Imahori, H.; Tkachenko, N. V.; Vehmanen, V.; Tamaki, K.; Lemmetyinen, H.; Sakata, Y.; Fukuzumi, S. *J. Phys. Chem. A* **2001**, *105*, 1750. (e) Vehmanen, V.; Tkachenko, N. V.; Imahori, H.; Fukuzumi, S.; Lemmetyinen, H. *Spectrochimica Acta, Part A* **2001**, *57*, 2229. (f) Imahori, H.; Yamada, H.; Guldi, D. M.; Endo, Y.; Shimomura, A.; Kundu, S.; Yamada, K.; Okada, T.; Sakata, Y.; Fukuzumi, S. *Angew. Chem., Int. Ed.* **2002**, *41*, 2344. (g) Kesti, T. J.; Tkachenko, N. V.; Vehmanen, V.; Yamada, H.; Imahori, H.; Fukuzumi, S.; Lemmetyinen, H. *J. Am. Chem. Soc.* **2002**, *124*, 8067. (h) Imahori, H.; Tamaki, K.; Araki, Y.; Sekiguchi, Y.; Ito, O.; Sakata, Y.; Fukuzumi, S. *J. Am. Chem. Soc.* **2002**, *124*, 5165.
(25) Guldi, D. M.; Asmus, K.-D. *J. Am. Chem. Soc.* **1997**, *119*, 5744.
(26) Yamada, H.; Imahori, H.; Nishimura, Y.; Yamazaki, I.; Fukuzumi, S. *Chem. Commun.* **2000**, 1921.
(27) Yamada, H.; Imahori, H.; Fukuzumi, S. *Adv. Mater.* **2002**, *14*, 892.

(28) Imahori, H.; El-Khouly, M. E.; Fujitsuka, M.; Ito, O.; Sakata, Y.; Fukuzumi, S. *J. Phys. Chem. A* **2001**, *105*, 325.
(29) Imahori, H.; Hagiwara, K.; Aoki, M.; Akiyama, T.; Taniguchi, S.; Okada, T.; Shirakawa, M.; Sakata, Y. *J. Am. Chem. Soc.* **1996**, *118*, 11771.
(30) (a) Tamaki, K.; Imahori, H.; Nishimura, Y.; Yamazaki, I.; Sakata, Y. *Chem. Commun.* **1999**, 625. (b) Luo, C.; Guldi, D. M.; Imahori, H.; Tamaki, K.; Sakata, Y. *J. Am. Chem. Soc.* **2000**, *122*, 6535. (c) Imahori, H.; Tamaki, K.; Guldi, D. M.; Luo, C.; Fujitsuka, M.; Ito, O.; Sakata, Y.; Fukuzumi, S. *J. Am. Chem. Soc.* **2001**, *123*, 2607.
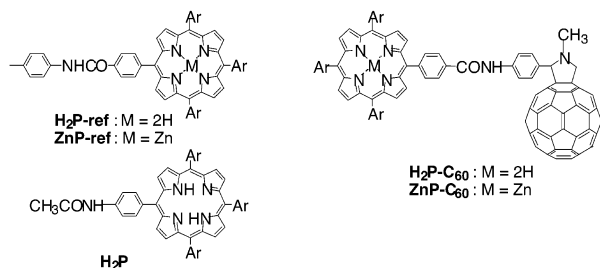
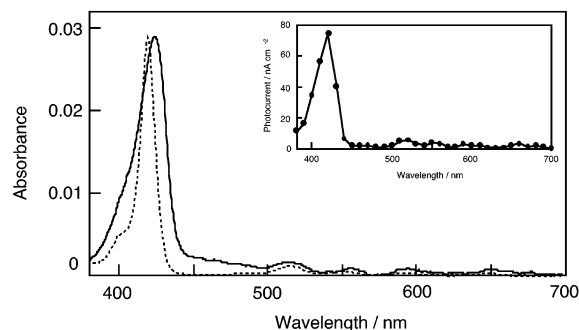**Figure 2.** Reference compounds used in this study.

Figure 3. UV–visible absorption spectra of **H₂P**/ITO (solid line) and **H₂P-ref** in THF (dotted line). The spectra are normalized at the Soret band for comparison. (Inset) Action spectrum of ITO/**H₂P**/TEA/Pt system; input power, 100 μW cm^{-2}; applied potential, +0.40 V vs Ag/AgCl (sat. KCl); an argon-saturated 0.1 M Na₂SO₄ aqueous solution containing 50 mM TEA.

H₂P-ref in THF. The Soret band of **H₂P**/ITO becomes broader than that of **H₂P-ref** in THF, whereas no appreciable change is seen in the Q-bands. The λ_{max} value of the Soret band of **H₂P**/ITO (425 nm) is red shifted by 5 nm as compared to that of **H₂P-ref** in THF (420 nm). Similar red shift (5 nm) was noted for the λ_{max} value of **H₂P**/Au (425 nm)[8c] relative to that of reference **H₂P** in THF (420 nm).[31] This indicates that the porphyrin environments of **H₂P**/ITO and **H₂P**/Au are similar and perturbed moderately within the monolayers, as compared to the references in THF, due to the aggregation.[8c]

The cyclic voltammetry measurements of **H₂P**/ITO and **H₂P-ref** in CH₂Cl₂ containing 0.2 M *n*-Bu₄NPF₆ were performed with a sweep rate of 0.10 V s^{-1} (electrode area, 0.48 cm^{-2}) to estimate the surface coverage (Figure 4). The cyclic voltammogram of **H₂P**/ITO is characterized by two successive anodic waves showing a well-defined current maximum but a much smaller coupled cathodic wave on the reversed scan at 0.10 V s^{-1} due to the instability of the radical cation. The anodic current increased linearly with increasing scan rate, implying that the porphyrin is a surface-confined electroactive molecule. The E^0_{ox} values [1.05, 1.34 V vs Ag/AgCl (sat. KCl)] were determined as the average of the anodic and cathodic peak potentials. The oxidation potentials of **H₂P-ref** in CH₂Cl₂ were also determined as E^0_{ox} = +1.04, +1.41 V versus Ag/AgCl (sat. KCl), which are similar to those of **H₂P**/ITO.[32] The adsorbed amounts (Γ) of **H₂P** on **H₂P**/ITO and on **H₂P**/Au were calculated from the

---

(31) The red shift and broadening of **H₂P**/Au were reported to be due to the partially stacked side-by-side porphyrin aggregation in the SAM;[8c] see: Khairutdinov, R. F.; Serpone, N. *J. Phys. Chem. B* **1999**, *103*, 761.

(32) Synthetic porphyrin dimers in close proximity generally exhibit a negative shift of the oxidation potential due to the interaction between the porphyrins.[8c] On the other hand, the decreased dielectric constant in the nonpolar monolayer as compared to that of bulk solution results in the positive shift of the oxidation potential of the porphyrin. Such compensation may be responsible for a small difference in the oxidation potential of the porphyrin in the monolayer and in the solution.[8c, 14b]
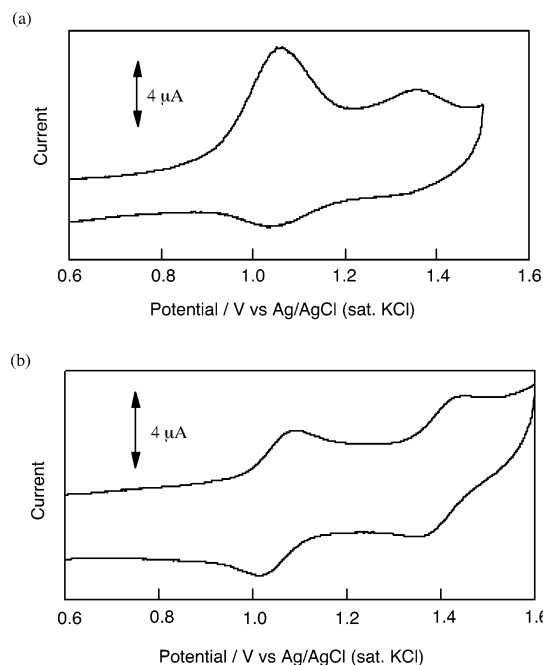
Figure 4. Cyclic voltammograms of (a) **H₂P**/ITO and (b) **H₂P-ref** in CH₂Cl₂ containing 0.2 M *n*-Bu₄NPF₆ with a sweep rate of 0.10 V s^{-1}; electrode area, 0.48 cm²; counter electrode, Pt wire; reference electrode, Ag/AgCl (sat. KCl).

first anodic peak currents of the porphyrin as 1.9 × 10^{-10} mol cm^{-2} (92 Å² molecule^{-1}) and 1.0 × 10^{-10} mol cm^{-2} (170 Å² molecule^{-1}),[8c] respectively, using a roughness factor of 1.3 for the ITO electrode from atomic force microscopy (AFM) measurements (*vide infra*) and 1.1 for gold electrode (see Experimental Section).[33] The Γ values thus determined are listed in Table 1.

To obtain further information on the surface structures of **H₂P**/ITO, **H₂P-C₆₀**/ITO, and ITO itself, we performed AFM measurements in air and in water with tapping mode (Nano-Scope IIIa, Digital Instruments). The ITO surface exhibits domain structures with a diameter of 10–100 nm and a height of ∼50 nm (see Supporting Information S9). After modification of ITO with **H₂P**, the ITO surface is covered uniformly with **H₂P** molecules, as shown in Figure 5a. This is consistent with the electrochemical results. It is interesting to note that when the surface of **H₂P**/ITO is measured in water, the aggregated structure of **H₂P** molecules is observed with a diameter of 20–30 nm (Figure 5b).

Anodic Photocurrent Generation in H₂P/ITO and H₂P/Au. Photoelectrochemical measurements were carried out in an argon-saturated 0.1 M Na₂SO₄ aqueous solution containing 50 mM triethanolamine (TEA) acting as an electron sacrificer using **H₂P**/ITO or **H₂P**/Au as the working electrode, a platinum counter electrode, and an Ag/AgCl (sat. KCl) reference electrode (hereafter represented by ITO/**H₂P**/TEA/Pt and Au/**H₂P**/TEA/Pt systems, respectively, where / denotes an interface). A stable anodic photocurrent from the electrolyte to the ITO electrode appeared immediately upon irradiation of the ITO electrode with λ = 419.5 ± 5.3 nm light with a power density of 100 μW cm^{-2} at an applied potential of +0.60 V vesrus Ag/AgCl (sat.

---

(33) When recalculated using the roughness factor 1.3 by AFM measurement, the Γ value of porphyrin SAM on ITO obtained in ref 26 is changed to 1.9 × 10^{-10} mol cm^{-2}.

Table 1. Surface Coverage, Fluorescence Lifetime, and Quantum Yield of Photocurrent Generation

system	surface coverage, $\Gamma^a/\times10^{-10}$ mol cm^{-2}	fluorescence lifetime,^{b} τ (relative amplitude)/ ns	quantum yield, $\phi^c/$ % TEA^d	quantum yield, $\phi^c/$ % HV$^{2+\,e}$
H$_2$P/ITO	1.9	1.0 (74%), 3.7 (26%)	3.4 ± 0.6	0.43 ± 0.02^i
H$_2$P/Au^f	1.0^f	0.015^f	0.012 ± 0.003	0.19 ± 0.10^i
H$_2$P		9.8^{f,g}		
H$_2$P-C$_{60}$/ITO	2.0	0.088 (91%), 0.43 (9%)		6.4 ± 2.3
H$_2$P-C$_{60}$		1.4 (88%), 2.7 (12%)^{g,h}		
H$_2$P-ref/ITO	1.4	1.2 (47%), 4.6 (57%)		0.21 ± 0.03
H$_2$P-ref		9.9^{g,h}		
ZnP-C$_{60}$/ITO	1.4	0.027 (98%), 0.23 (2%)		3.9 ± 1.1
ZnP-C$_{60}$		0.075^{g,h}		
ZnP-ref/ITO	0.7	0.089 (77%), 0.31 (23%)		0.36 ± 0.06
ZnP-ref		2.1^{g,h}		
H$_2$P-ref/Au		0.040^f		

^{a} Obtained from the area of the anodic peak due to the first porphyrin oxidation using cyclic voltammetry. ^{b} Obtained using a single photon counting technique when excited at 435 nm and monitored at 655 nm for freebase porphyrins and 605 nm for zinc porphyrins. ^{c} Obtained in the standard three electrode systems. The quantum yields of the photocurrent generation were obtained by the following equation: $\phi = (i/e)/[I(1 - 10^{-A})]$, where $I = (W\lambda)/(hc)$, i is the photocurrent density, e is the elementary charge, I is number of photons per unit area and unit time, λ is the wavelength of light irradiation, A is absorbance of the adsorbed dyes at λ nm, W is light power irradiated at λ nm, c is the light velocity, and h is the Planck constant. ^{d} Argon-saturated 0.1 M Na$_2$SO$_4$ aqueous solution containing 50 mM TEA; excitation with light at $\lambda = 419.5 \pm 5.3$ nm with 1 mW cm^{-2} at bias of +0.40 V vs Ag/AgCl (saturated KCl). ^{e} Oxygen-saturated 0.1 M Na$_2$SO$_4$ aqueous solution containing 5 mM HV^{2+}; excitation with $\lambda = 430.0 \pm 5.0$ nm light with 500 μW cm^{-2} at bias of -0.20 V vs Ag/AgCl (saturated KCl). ^{f} From ref 8c. ^{g} In THF. ^{h} From ref 13d. ^{i} 5 mM MV^{2+} was used instead of HV^{2+} with excitation wavelength of $\lambda = 419.5 \pm 5.3$ nm.

Figure 5. Tapping mode atomic force micrography of **H$_2$P**/ITO (a) in air (Z range: 2 nm) and (b) in water (40 nm) and of (c) **H$_2$P-C$_{60}$**/ITO in air (0.4 nm). The color scale represents the height topography, with bright and dark representing the highest and lowest features, respectively.

KCl) as shown in Figure 6a. The photocurrent fell down instantly when the illumination was cut off. There is a good linear relationship between the photocurrent intensity and the light intensity at each wavelength (from 0.10 to 6.0 mW cm^{-2}). In the absence of TEA, the anodic photocurrent was negligible under otherwise the same experimental conditions. Further addition of TEA (>50 mM) into the electrolyte solution did not increase the photocurrent.[34] The anodic photocurrent increases monotonically with increasing positive bias to the ITO electrode [from -0.20 to $+0.40$ V vs Ag/AgCl (sat. KCl)], whereas the dark current remains constant, as shown in Figure 6b. The agreement of the action spectrum with the absorption spectrum of **H$_2$P**/ITO in 380–700 nm (Figure 3) demonstrates clearly that the porphyrin is the photoactive species responsible for the photocurrent generation. These results demonstrate that photocurrent flows from the electrolyte to the ITO electrode via the excited state of the porphyrin SAM.

Similar photoelectrochemical behavior was observed for the corresponding porphyrin SAMs on the gold electrode, denoted as an Au/**H$_2$P**/TEA/Pt system. The quantum yields of photocurrent generation were compared between the Au/**H$_2$P**/TEA/Pt and ITO/**H$_2$P**/TEA/Pt systems at an applied potential of +0.40 V versus Ag/AgCl (sat. KCl) where dark current is negligible. The quantum yields (ϕ) based on the number of photons absorbed by **H$_2$P** on **H$_2$P**/ITO and that on **H$_2$P**/Au were calculated using the input power ($\lambda = 419.5 \pm 5.3$ nm light of
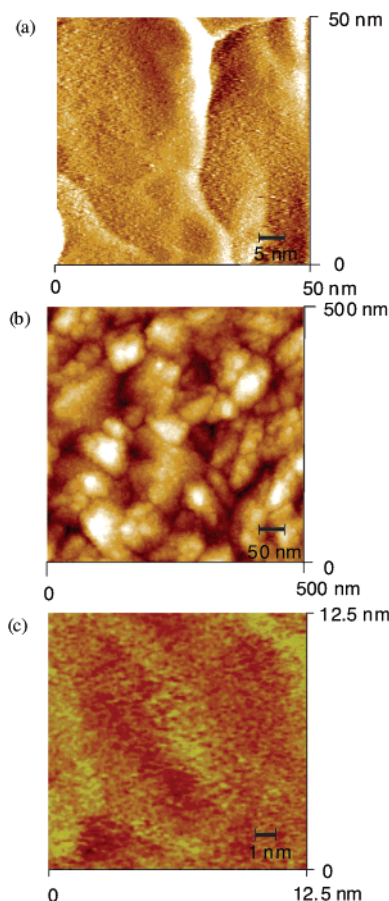
1 mW cm^{-2}), the photocurrent density, and the absorbance on the electrodes (ITO/**H$_2$P**/TEA/Pt system: $i = 740$ nA cm^{-2}, $A = 0.029$. Au/**H$_2$P**/TEA/Pt system: $i = 2.8$ nA cm^{-2}, $A = 0.030$). The ϕ value ($3.4 \pm 0.6\%$) of the ITO/**H$_2$P**/TEA/Pt system is ca. 280 times larger than the ϕ value ($0.012 \pm 0.003\%$) of the Au/**H$_2$P**/TEA/Pt system (Table 1).

Such a remarkable difference in the quantum yields of photocurrent generation may stem from the difference in the photophysical properties between the **H$_2$P**/ITO and **H$_2$P**/Au systems. Thus, we performed time-correlated, single-photon counting fluorescence measurements on **H$_2$P**/ITO and **H$_2$P**/Au as well as **H$_2$P-ref** and **H$_2$P** in solutions with the excitation wavelength at 435 nm. In each case, the decay of the fluorescence intensity due to the porphyrin excited singlet state (^{1}P*) was monitored at 655 nm. The decay curve could be well fitted as a single exponential except for the case of **H$_2$P**/ITO, and the fluorescence lifetimes (τ) are summarized in Table 1. The τ values of **H$_2$P**/ITO [$\tau = 1.0$ ns (74%), 3.7 ns (26%)] are significantly longer than the value of **H$_2$P**/Au ($\tau = 15$ ps)[8c] but shorter than those of **H$_2$P-ref** ($\tau = 9.9$ ns)[13d] and **H$_2$P** ($\tau = 9.8$ ns)[8c] in THF. We have previously reported that the energy transfer (EN) quenching of the porphyrin singlet excited state (^{1}H$_2$P*) by the gold surface is responsible for the extremely short

(34) TEA may form a complex with the porphyrin SAM on ITO electrode, when the rate of photoinduced electron transfer from TEA to the excited state of porphyrin SAM becomes independent of TEA concentration.
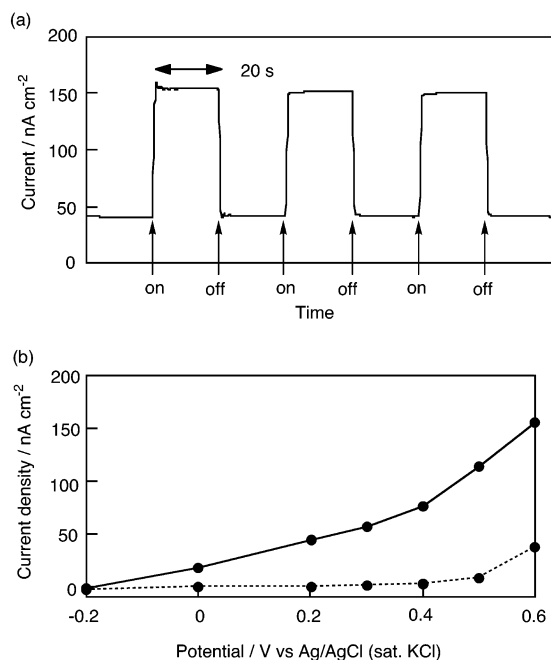
(a)

(b)

Figure 6. (a) Photoelectrochemical response of an ITO/**H₂P**/TEA/Pt cell; applied potential, +0.60 V vs Ag/AgCl (sat. KCl). (b) Photocurrent vs applied potential curves for an ITO/**H₂P**/TEA/Pt system (solid line with closed circles). The dark currents are shown as a dotted line with closed circles. The data are the averages of six samples. $\lambda = 419.5 \pm 5.3$ nm (100 μW cm^{-2}); an argon-saturated 0.1 M Na₂SO₄ aqueous solution containing 50 mM TEA.
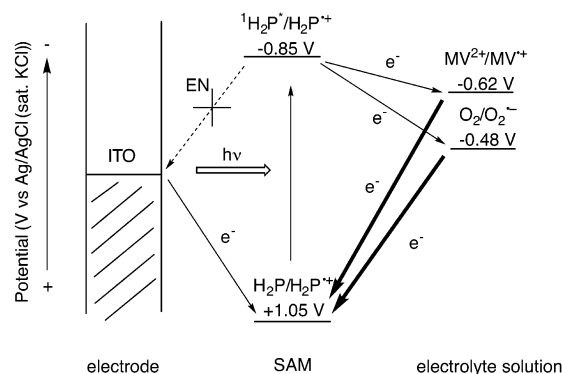
Scheme 1
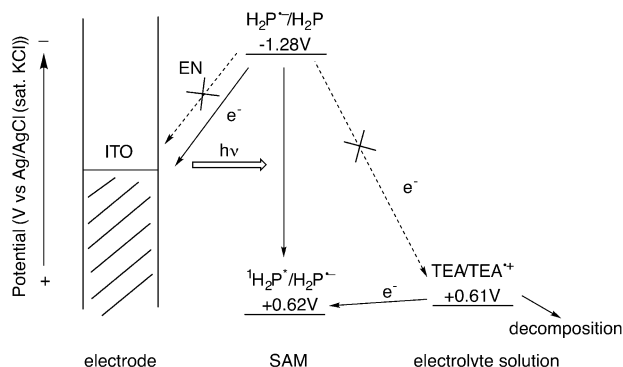
lifetime of the porphyrin on the gold surface.[8c] Thus, the data in Table 1 clearly indicate that the EN quenching efficiency of $^1P^*$ on the ITO electrode is much suppressed as compared to that on the gold surface.

Based on the energetics of the photoactive and radical ion species involved in the ITO/**H₂P**/TEA/Pt system, the mechanism of photocurrent generation in **H₂P**/ITO is shown in Scheme 1. First, an ET takes place from TEA [+0.61 V vs Ag/AgCl (sat. KCl)][11d] to the singlet excited state $^1H_2P^*$ [+0.62 V vs Ag/AgCl (sat. KCl)][8c] rather than the excited triplet state $^3H_2P^*$ [+0.12 V vs Ag/AgCl (sat. KCl)],[8c] yielding the porphyrin radical anion (H₂P$^{\bullet-}$) and TEA radical cation (TEA$^{\bullet+}$). TEA$^{\bullet+}$ thus formed is known to undergo irreversible decomposition via hydrogen abstracting rearrangement from another TEA,[35]

(35) (a) Chan, S.-F.; Chou, M.; Creutz, C.; Matsubara, T.; Sutin, N. *J. Am. Chem. Soc.* **1981**, *103*, 369. (b) Downard, A. J.; Surridge, N. A.; Gould, S.; Meyer, T. J.; Deronzier, A.; Moutet, J.-C. *J. Phys. Chem.* **1990**, *94*, 6754. (c) Matsuoka, S.; Yamamoto, K.; Ogata, T.; Kusaba, M.; Nakashima, N.; Fujita, E.; Yanagida, S. *J. Am. Chem. Soc.* **1993**, *115*, 601. (d) Aoki, A.; Abe, Y.; Miyashita, T. *Langmuir* **1999**, *15*, 1463.

Scheme 2

which suppresses charge recombination (CR) from H₂P$^{\bullet-}$ to TEA$^{\bullet+}$. Photogenerated H₂P$^{\bullet-}$ [−1.28 V vs Ag/AgCl (sat. KCl)] gives an electron to the ITO electrode, resulting in the anodic photocurrent generation. In such a case, the rate-determining step for the photocurrent generation may be the photoinduced electron transfer from TEA to $^1H_2P^*$, when the quantum yield for photocurrent generation is significantly dependent on the excited-state lifetime. In fact, the ϕ value in **H₂P**/ITO is much larger than that in **H₂P**/Au because of the suppression of undesirable EN quenching of $^1H_2P^*$ by the ITO electrode as compared to the **H₂P**/Au system. The relative ratio (110) of the weighted average lifetimes of **H₂P**/ITO ($\tau = 1.7$ ns) versus **H₂P**/Au ($\tau = 15$ ps) is indeed consistent with the corresponding ratio (280) of the quantum yields of the two systems.

Cathodic Photocurrent Generation in H₂P/ITO and H₂P/Au. Since it is desirable to construct a photoelectrochemical cell without a sacrificial electron donor such as TEA, we have also examined cathodic photocurrent generation in **H₂P**/ITO and **H₂P**/Au in the presence of oxygen and methyl viologen (MV^{2+}) acting as an electron mediator (acceptor) in the electrolyte solution (hereafter represented by ITO/**H₂P**/MV^{2+}/Pt and Au/**H₂P**/MV^{2+}/Pt systems, respectively, where / denotes an interface). The optimized experimental conditions (an oxygen-saturated 0.1 M Na₂SO₄ aqueous solution containing 5 mM methyl viologen) have been well established for a series of porphyrin SAM on the gold electrode,[8c,13d,14b] in which cathodic photocurrent generation was observed under illumination ($\lambda = 419.5 \pm 5.3$ nm light of 100 μW cm^{-2}) at an applied potential of −0.20 V versus Ag/AgCl (sat. KCl). The quantum yield of photocurrent generation in the ITO/**H₂P**/MV^{2+}/Pt system (0.43 $\pm$ 0.02%) is larger than that in the Au/**H₂P**/MV^{2+}/Pt system (0.19 $\pm$ 0.10%). In this case as well, the ITO electrode is superior to the Au electrode. As compared to the 280 times improvement of the ϕ value of the anodic photocurrent generation in the ITO/**H₂P**/TEA/Pt system relative to the Au/**H₂P**/TEA/Pt system (*vide supra*), however, the ϕ value of the ITO/**H₂P**/MV^{2+}/Pt system is only 2 times larger than the value of the Au/**H₂P**/MV^{2+}/Pt system despite the large difference of fluorescence lifetimes between **H₂P**/ITO and **H₂P**/Au.

The mechanism of cathodic photocurrent generation in ITO/**H₂P**/MV^{2+}/Pt system is shown in Scheme 2, which is different from the mechanism of anodic photocurrent generation in Scheme 1. When the potentials of the porphyrin singlet excited state [$^1H_2P^*/H_2P^{\bullet+} = -0.85$ V vs Ag/AgCl (sat. KCl)][8c] and the triplet state [$^3H_2P^*/H_2P^{\bullet+} = -0.35$ V vs Ag/AgCl (sat. KCl)] are taken into account,[8c] photoirradiation of the modified ITO electrode results in intermolecular ET from $^1H_2P^*$ (not $^3H_2P^*$)

to MV^{2+} [$E^0_{red} = -0.62$ V vs Ag/AgCl (sat. KCl)][8c] or O_2 [$E^0_{red} = -0.48$ V vs Ag/AgCl (sat. KCl)].[8c] The reduced electron carrier ($MV^{•+}$ or $O_2^{•-}$) diffuses to release an electron to the platinum counter electrode, whereas the resultant porphyrin radical cation [$H_2P/H_2P^{•+} = 1.05$ V vs Ag/AgCl (sat. KCl)] captures an electron from the ITO electrode, generating the cathodic current flow (Scheme 2). The electron transfer from the ITO electrode to $H_2P^{•+}$ may be rather slow as compared to the gold electrode.[36] Thus, CR would occur efficiently from $MV^{•+}$ or $O_2^{•-}$ to $H_2P^{•+}$ to decrease the quantum yields of cathodic photocurrent generation in the ITO/H_2P/MV^{2+}/Pt system.[35d] The relatively slow electron transfer from the ITO electrode to $H_2P^{•+}$ may be responsible for the less remarkable enhancement of the ϕ value of the cathodic photocurrent generation of the ITO/H_2P/MV^{2+}/Pt system versus the Au/H_2P/MV^{2+}/Pt system (only two times) as compared with the 280 times enhancement of the ϕ value in the anodic photocurrent generation of the ITO/H_2P/TEA/Pt system versus the Au/H_2P/TEA/Pt system. In the case of the anodic photocurrent generation in the ITO/H_2P/TEA/Pt system, the CR from $H_2P^{•-}$ to TEA$^{•+}$ was suppressed by the facile irreversible decomposition of TEA$^{•+}$ (Scheme 1). Similar difference in the photocurrent behavior between TEA and MV^{2+} was reported in LB films of Ru(bpy)$_3^{2+}$ copolymer on ITO in the presence of TEA or MV^{2+}.[35d]

Porphyrin–Fullerene SAMs on ITO and Gold Electrodes. As described above, the ITO electrode is superior to the gold electrode because of the less EN quenching of $^1H_2P^*$ as compared to the gold electrode. This superiority of the ITO electrode is partially canceled by the relatively slow electron transfer from the ITO electrode to $H_2P^{•+}$ as compared to the gold electrode, which results in a decrease in the anodic photocurrent generation due to the competing CR process. However, the CR process from $MV^{•+}$ or $O_2^{•-}$ to $H_2P^{•+}$ in ITO/H_2P/MV^{2+}/Pt in Scheme 2 may be suppressed by replacing the single chromophore (H_2P) SAMs with SAMs of porphyrin linked with an electron acceptor. Thus, C_{60} (an acceptor) is linked with porphyrin SAMs on ITO (H_2P-C_{60}//ITO and **ZnP-C$_{60}$**/ITO) to examine the cathodic photocurrent generation in comparison with the reference porphyrin SAMs with a spacer of the same number of atoms (**H$_2$P-ref**/ITO and **ZnP-ref**/ITO) and those with **H$_2$P-ref**/Au in Figure 1.

Absorption spectra of **H$_2$P-C$_{60}$**/ITO and **H$_2$P-ref**/ITO were compared to those of **H$_2$P-C$_{60}$** and **H$_2$P-ref** in THF (Figure 7). The Soret bands of **H$_2$P-C$_{60}$**/ITO and **H$_2$P-ref**/ITO become broader than those of **H$_2$P-C$_{60}$** and **H$_2$P-ref** in THF. The λ_{max} values of the Soret bands of **H$_2$P-C$_{60}$**/ITO (426 nm) and **H$_2$P-ref**/ITO (426 nm) are red shifted by 6 nm relative to those of **H$_2$P-C$_{60}$** (420 nm) and **H$_2$P-ref** (420 nm) in THF, respectively. Similar red shift and broadening of the Soret bands were observed for **ZnP-C$_{60}$**/ITO (5 nm) and **ZnP-ref**/ITO (7 nm) relative to **ZnP-C$_{60}$** and **ZnP-ref** in THF, respectively. These results indicate that the porphyrin environments of **H$_2$P-C$_{60}$**/ITO and **ZnP-C$_{60}$**/ITO are similar to those of the corresponding reference systems without C_{60} (**H$_2$P-ref**/ITO and **ZnP-ref**/ITO) and perturbed moderately, relative to the references in THF, due to the porphyrin aggregation, as observed in the case of **H$_2$P**/ITO and **H$_2$P**/Au (*vide supra*).[8c]
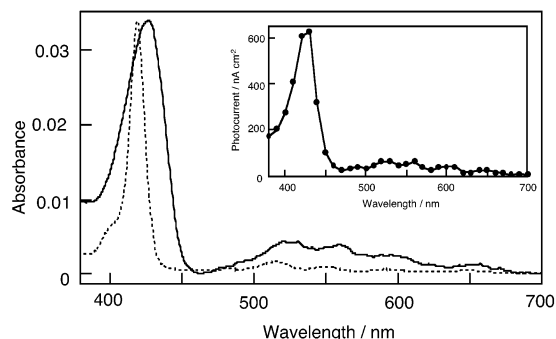

Figure 7. UV–visible absorption spectra of **H$_2$P-C$_{60}$**/ITO (solid line) and **H$_2$P-C$_{60}$** in THF (dotted line). The spectra are normalized at the Soret band for comparison. (Inset) Action spectrum of ITO/**H$_2$P-C$_{60}$**/HV^{2+}/Pt system; input power, 500 μW cm^{-2}; applied potential, -0.10 V vs Ag/AgCl (sat. KCl); an oxygen-saturated 0.1 M Na$_2$SO$_4$ aqueous solution containing 5 mM HV^{2+}.

The cyclic voltammetric measurements of **H$_2$P-C$_{60}$**/ITO and **H$_2$P-C$_{60}$** in CH$_2$Cl$_2$ containing 0.2 M *n*-Bu$_4$NPF$_6$ electrolyte were performed with a sweep rate of 0.10 V s^{-1} (electrode area, 0.48 cm^{-2}) to estimate the surface coverage (see Supporting Information S10). The electrochemical behavior of **H$_2$P-C$_{60}$**/ITO is similar to that of **H$_2$P**/ITO (*vide supra*). The cyclic voltammogram of **H$_2$P-C$_{60}$**/ITO is characterized by two successive anodic waves showing a well-defined current maximum but much smaller coupled cathodic wave on the reversed scan at 0.10 V s^{-1} due to the instability of the radical cation. The E^0_{ox} values were determined as 1.10 and 1.38 V versus Ag/AgCl (sat. KCl). The oxidation potentials of **H$_2$P-C$_{60}$** in the CH$_2$Cl$_2$ solution were also determined as $E^0_{ox} = +1.05$, 1.30 V versus Ag/AgCl (sat. KCl),[13d] which are shifted to the negative direction compared to that of **H$_2$P-C$_{60}$**/ITO. This difference can be explained as a consequence of the decreased dielectric constant in the nonpolar monolayer as compared to that of bulk solution rather than interaction between the porphyrin molecules.[8c,13d,32] Similar electrochemical behavior was noted for **ZnP-C$_{60}$**/ITO, **H$_2$P-ref**/ITO, and **ZnP-ref**/ITO. The adsorbed amounts (Γ) of **P-C$_{60}$** on **P-C$_{60}$**/ITO and **P-ref** on **P-ref**/ITO (P=H$_2$P or ZnP) were calculated from the anodic peak of the porphyrin using a roughness factor of 1.3 from atomic force microscopy (AFM) measurements (*vide supra*) and summarized in Table 1. The Γ value of **H$_2$P-C$_{60}$**/ITO (2.0 $\times$ 10^{-10} mol cm^{-2}) is virtually the same as the value of **H$_2$P**/ITO (1.9 $\times$ 10^{-10} mol cm^{-2}) and those of a well-packed ferrocene–porphyrin–fullerene triad SAM (1.9 $\times$ 10^{-10} mol cm^{-2})[13d] and porphyrin SAM (1.5 $\times$ 10^{-10} mol cm^{-2}) on Au(111).[8c] The Γ values of **ZnP-C$_{60}$**/ITO (1.4 $\times$ 10^{-10} mol cm^{-2}) and **ZnP-ref**/ITO (0.7 $\times$ 10^{-10} mol cm^{-2}) are significantly smaller than those of **H$_2$P-C$_{60}$**/ITO and **H$_2$P-ref**/ITO, respectively. This implies that some porphyrins and porphyrin–fullerene dyads were lost from the surfaces of the ITO during metalation.[13d,37]

To obtain further information on the surface structures of **H$_2$P-C$_{60}$**/ITO, we performed AFM measurements in air with tapping mode (Figure 5c).[27] After modification of ITO with **H$_2$P-C$_{60}$**, the ITO surface is covered uniformly. It should be emphasized here that aggregation of bright spots observed within a domain corresponds to well-packed structures of **H$_2$P-C$_{60}$** molecules with a separation of ∼1 nm, which agrees with the

(36) The ET rate constant between ferrocene and gold electrode with a spacer of the same number atoms was reported to be 1.5 × 10^4 s^{-1}; see: Weber, K.; Hockett, L.; Creager, S. *J. Phys. Chem. B* **1997**, *101*, 8286.

(37) McCallien, D. W. J.; Burn, P. L.; Anderson, H. L. *J. Chem. Soc., Perkin Trans. 1* **1997**, 2581.
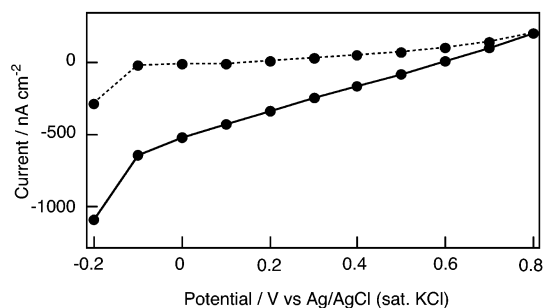
Figure 8. Photocurrent vs applied potential curves for ITO/**H₂P-C₆₀**/HV²⁺/ Pt system (solid line with closed circles): $\lambda = 430.0 \pm 5.0$ nm (500 μW cm⁻²); an oxygen-saturated 0.1 M Na₂SO₄ aqueous solution containing 5 mM HV²⁺. The dark currents are shown as dotted lines with closed circles. The data are the averages of three samples.

diameter of C_{60}. To the best of our knowledge, this is the first observation of self-assembled molecules on ITO in molecular resolution.

Photoelectrochemical measurements were carried out in a 0.1 M Na₂SO₄ aqueous solution using **H₂P-C₆₀**/ITO or **ZnP-C₆₀**/ ITO as a working electrode, a Pt counter electrode, and an Ag/ AgCl (sat. KCl) reference electrode. A stable cathodic photocurrent appeared immediately upon irradiation of the **H₂P-C₆₀**/ ITO electrode with $\lambda = 430.0 \pm 5.0$ nm light with 500 μW cm⁻² at an applied potential of -0.20 V versus Ag/AgCl (sat. KCl) in an argon-saturated 0.1 M Na₂SO₄ aqueous solution. When the irradiation was cut off, the photocurrent fell down instantly. The effects of oxygen [-0.48 V vs Ag/AgCl (sat. KCl)][8c,13d,14b] and 1,1-dihexyl-4,4′-dipyridinium diperchlorate (HV²⁺) [-0.24 V vs Ag/AgCl (sat. KCl)] as an electron carrier on the photoelectrochemical properties were also examined to optimize the photocurrent generation.[38] The cathodic photocurrent increased gradually with bubbling oxygen into the electrolyte solution. Under the oxygen-saturated conditions, the photocurrent increased linearly with an increase in HV²⁺ concentration to reach a constant value at around 5 mM of HV²⁺ as an electron carrier (See Supporting Information S11). These results are consistent with the fact that methyl viologen [-0.62 V vs Ag/AgCl (sat. KCl)] and O₂ [-0.48 V vs Ag/AgCl (sat. KCl)] acts as electron acceptors in similar photoelectrochemical systems.[8c] Such a saturated behavior was also reported for porphyrin−alkanethiol mixed SAMs on gold electrodes in the presence of MV²⁺.[14b,39,40] There is a good linear relationship between the photocurrent and the light intensity at each wavelength (from 0.10 to 6.0 mW cm⁻²). The net photocurrent relative to the dark current decreased monotonically with increasing positive bias (from -0.20 to $+0.80$ V vs Ag/AgCl) and disappeared at $+0.80$ V versus Ag/AgCl (sat. KCl) (Figure 8). Similar photoelectrochemical behavior was observed for the reference systems: **H₂P-ref**/ITO, **ZnP-C₆₀**/ITO, and **ZnP-ref**/ ITO.

The quantum yields of the photocurrent generation (hereafter denoted as ITO/**H₂P-C₆₀**/HV²⁺/Pt system) were determined under the optimized conditions [0.1 M Na₂SO₄ aqueous solution containing 5 mM HV²⁺ under irradiation of the **H₂P-C₆₀**/ITO electrode with $\lambda = 430.0 \pm 5.0$ nm light with 500 μW cm⁻² at an applied potential of -0.20 V versus Ag/AgCl (sat. KCl)] based on the input power, the photocurrent density, and the absorbance on the electrodes (ITO/**H₂P-C₆₀**/HV²⁺/Pt system: $i = 810$ nA cm⁻², $A = 0.033$. ITO/**ZnP-C₆₀**/HV²⁺/Pt system: $i = 450$ nA cm⁻², $A = 0.030$. ITO/**H₂P-ref**/HV²⁺/Pt system: $i = 24$ nA cm⁻², $A = 0.030$. ITO/**ZnP-ref**/HV²⁺/Pt system: $i = 39$ nA cm⁻², $A = 0.028$) at the applied potential. The quantum yield of the photocurrent generation of the ITO/**H₂P-C₆₀**/HV²⁺/ Pt system ($6.4 \pm 2.3\%$) is 30 times larger than that of the ITO/ **H₂P-ref**/HV²⁺/Pt system ($0.21 \pm 0.03\%$). The agreement of absorption and action spectra (380−700 nm) of **H₂P-C₆₀**/ITO (Figure 7) reveals that the porphyrin is the major photoactive species responsible for the photocurrent generation. Similar photoelectrochemical behavior was observed for the ITO/**ZnP-C₆₀**/HV²⁺/Pt system. There is also a good agreement between the absorption spectrum of **ZnP-C₆₀**/ITO and action spectrum of the ITO/**ZnP-C₆₀**/HV²⁺/Pt system. The quantum yield of the photocurrent generation of the ITO/**ZnP-C₆₀**/HV²⁺/Pt system ($3.9 \pm 1.1\%$) is 11 times larger than that of the ITO/**ZnP-ref**/ HV²⁺/Pt system ($0.36 \pm 0.06\%$). These results clearly show that remarkable enhancement of the photocurrent generation in the present systems results from an incorporation of the C_{60} moiety as an electron acceptor into the porphyrin SAMs on the ITO.

The fluorescence lifetimes on the ITO surfaces were measured by a picosecond single-photon counting technique at emission wavelengths of 655 nm for **H₂P-C₆₀**/ITO and **H₂P-ref**/ITO (Figure 9a) and 605 nm for **ZnP-C₆₀**/ITO and **ZnP-ref**/ITO due to the porphyrin moiety with excitation at 425 nm. The decay curve of the fluorescence intensity could be fitted as double exponentials, and the fluorescence lifetimes thus determined are listed in Table 1. The weighted average fluorescence lifetimes of **H₂P-C₆₀**/ITO (0.12 ns) and **ZnP-C₆₀**/ITO (0.031 ns) are much shorter than those of **H₂P-ref**/ITO (3.2 ns) and **ZnP-ref**/ITO (0.14 ns), respectively. This can be ascribed to the strong quenching of the porphyrin singlet excited states by the attached C_{60} moiety via intramolecular ET on the ITO surface.[13d,e] It should be emphasized that the fluorescence lifetime of **H₂P-ref**/ITO (3.2 ns) is 80 times longer than that of the porphyrin SAM (**H₂P-ref**/Au in Figure 1) with a similar length of the spacer on the gold surface (40 ps; shown in Figure 9b)[8c] but ¹/₃ times shorter than that of the porphyrin reference (**H₂P-ref**) in solutions (9.9 ns in THF).[8c] Since the fluorescence lifetimes of **H₂P-ref** on the glass slide and of **H₂P-ref**/ITO are similar, the moderate fluorescence lifetime of **H₂P-ref**/ITO can be attributed to the self-quenching of the porphyrins due to the aggregation as in the case of **H₂P**/ITO (*vide supra*).[36,41,42]

The femtosecond time-resolved transient absorption spectrum of **H₂P-C₆₀**/ITO with an excitation wavelength of 400 nm was

(38) For the improvement of the quantum yield of the photocurrent generation, we employed different experimental conditions [i.e., changing the electrolyte solutions (CH₃CN containing 0.1 M *n*-Bu₄NPF₆) and the electron acceptors (*p*-benzoquinone, 2-chloro-*p*-benzoquinone, and 2,5-dichloro-*p*-benzo-quinone, and 9-phenyl-10-methylacridinium perchlorate)]. However, the quantum yields were lower than the present optimized conditions using HV²⁺ and O₂ as electron acceptors.

(39) Andersson, M.; Davidsson, J.; Hammarström, L.; Korppi-Tommola, J.; Peltola, T. *J. Phys. Chem. B* **1999**, *103*, 3258.

(40) This may be ascribed to association between the porphyrin and hexyl viologen, in which the hexyl moiety might be buried within the hydrophobic SAM at the assembly solution interface; see: Creager, S. E.; Collard, D. M.; Fox, M. A. *Langmuir* **1990**, *6*, 1617.

(41) Akins, D. L.; Özçelik, S.; Zhu, H.-R.; Guo, C. *J. Phys. Chem.* **1996**, *100*, 14390.

(42) The short fluorescence lifetimes of **ZnP-ref**/ITO (0.089 ns, 0.31 ns) relative to **H₂P-ref**/ITO (1.2 ns, 4.6 ns) can be attributed to the strong self-quenching of the zinc porphyrin due to the intensive aggregation between the porphyrins as well as the intrinsic short fluorescence lifetime of **ZnP-ref** (2.1 ns in THF) as compared to that of **H₂P-ref** (9.9 ns in THF).

(a)

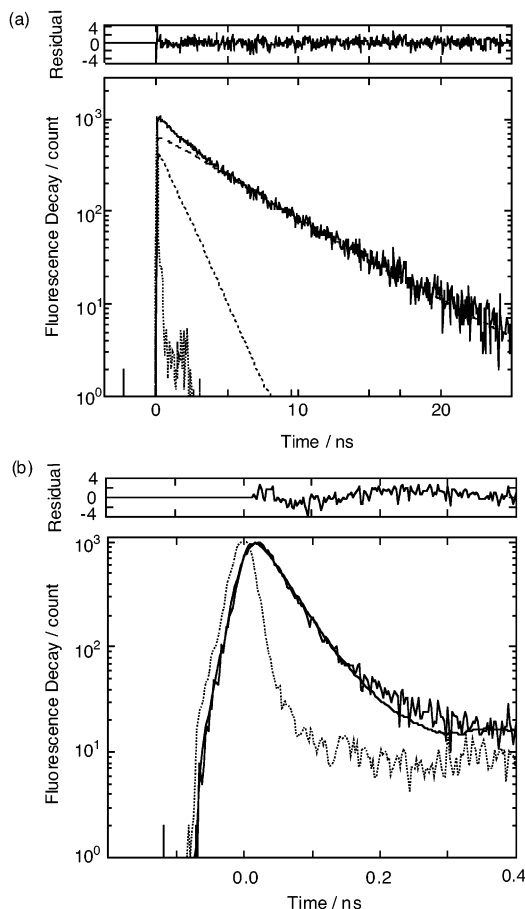(b)

Figure 9. Fluorescence decay curves of (a) **H₂P-ref**/ITO and (b) **H₂P-ref**/Au in THF observed at 655 nm by the single-photon counting method. The excitation wavelength is 425 nm for **H₂P-ref**/ITO and 435 nm for **H₂P-ref**/Au.
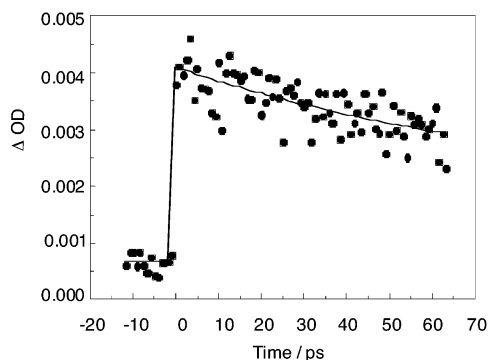

**Figure 10.** Time profile of **H₂P-C₆₀**/ ITO at 430 nm after photoexcitation at 400 nm.

also measured to confirm the photoinduced ET from the porphyrin excited singlet state to the C_{60} moiety on ITO. The ground state bleaching recovery at 430 nm due to the porphyrin excited singlet state (Figure 10) could be fitted as three exponential components [88 ps (42%), 800 ps (45%), >2 ns (13%)]. The fast decay component is in good agreement with the fluorescence lifetime of **H₂P-C₆₀**/ITO (88 ps), demonstrating the photoinduced ET process on ITO.[43]

Based on the above results together with the well-established photodynamics of porphyrin−fullerene linked systems on electrodes[13] as well as those of **H₂P-C₆₀** and **ZnP-C₆₀** in solutions,[28,29] the mechanism of enhanced photocurrent generation

Scheme 3
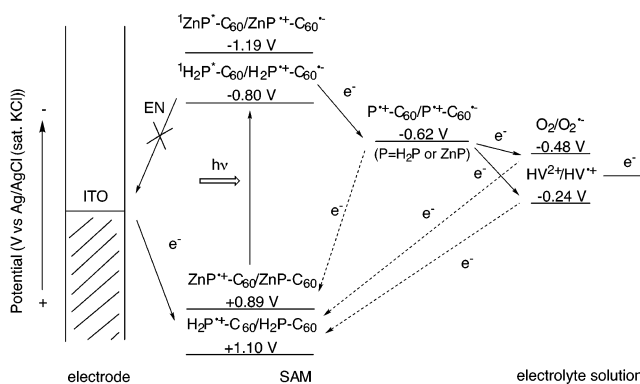
in the ITO/**H₂P-C₆₀**/HV^{2+}/Pt system and ITO/**ZnP-C₆₀**/HV^{2+}/Pt system is summarized in Scheme 3. First, an intramolecular ET takes place from $^1P^*$ [H_2P, −0.80 V; ZnP, −1.19 V vs Ag/AgCl (sat. KCl)][13] to C_{60}, followed by intermolecular ET from the resulting $C_{60}^{\bullet-}$ [−0.62 V vs Ag/AgCl (sat. KCl)][13] to an electron carrier, O_2 [−0.48 V vs Ag/AgCl (sat. KCl)][13] or HV^{2+} [−0.24 V vs Ag/AgCl (sat. KCl)].[13] The quantum yield of the ITO/**ZnP-C₆₀**/HV^{2+}/Pt system (3.9%) is lower than that of the ITO/**H₂P-C₆₀**/HV^{2+}/Pt system (6.4%) despite the efficient quenching of the zinc porphyrin excited singlet state ($^1ZnP^*$) of **ZnP-C₆₀** (i.e., 75 ps) relative to **ZnP-ref** (2.1 ns) in THF (Table 1). Judging from the relative ratios of the fluorescence lifetimes of **H₂P-C₆₀**/ITO versus **H₂P-ref**/ITO and **ZnP-C₆₀**/ITO versus **ZnP-ref**/ITO, we believed the self-quenching of the zinc porphyrin excited singlet state ($^1ZnP^*$) in the ITO/**ZnP-C₆₀**/HV^{2+}/Pt cell may result in the deactivation of $^1ZnP^*$ to reduce the quantum yield of the photocurrent generation.

The intermolecular ET rate from $C_{60}^{\bullet-}$ to HV^{2+} is estimated as $\sim 5 \times 10^7$ s^{-1} at the concentration of HV^{2+} (~ 5 mM) assuming the photoinduced ET rate constant is diffusion-limited ($\sim 10^{10}$ M^{-1} s^{-1}). Thus, the intermolecular ET ($\sim 5 \times 10^7$ s^{-1}) can compete well with the charge recombination of **H₂P•⁺-C₆₀•⁻** (2.2×10^7 s^{-1} in benzonitrile)[29] and **ZnP•⁺-C₆₀•⁻** (1.3×10^6 s^{-1} in benzonitrile).[28] On the other hand, an electron is injected from the ITO to $P^{\bullet+}$ [H_2P, +1.10 V; ZnP, +0.89 V vs Ag/AgCl (sat. KCl)], which eventually leads to the cathodic current generation. In contrast with the case of the C_{60}-linked system in Scheme 3, the photocurrent generation in the reference systems without C_{60} (ITO/**H₂P-ref**/HV^{2+}/Pt and ITO/**ZnP-ref**/HV^{2+}/Pt systems) is much reduced due to the less efficient intermolecular ET from $^1P^*$ to HV^{2+} as compared to the intramolecular ET in the C_{60} linked system.[44]

Conclusions

We have successfully demonstrated that the quantum yield of photocurrent generation for the porphyrin SAM cell on ITO

(43) Characteristic absorption due to H_2P radical cation (around 660 nm) and C_{60} radical anion (around 1000 nm) could not be confirmed because of the poor signal-to-noise ratio. The input laser power was minimized to avoid exciton−exciton annihilation processes which occur dominantly within a few picoseconds after laser excitation with high power.

(44) The quantum yields of the photocurrent generation in the ITO/**ZnP-ref**/HV^{2+}/Pt system (0.36%) is larger than that of the ITO/**H₂P-ref**/HV^{2+}/Pt system (0.21%), because of the strong quenching of the porphyrin excited state of **ZnP-ref**/ITO (weighted average fluorescence lifetime = 0.14 ns) as compared to that of **H₂P-ref**/ITO (3.2 ns). This can be ascribed to the large free energy change for photoinduced ET from $^1ZnP^*$ to HV^{2+} (0.95 eV) relative to that from $^1H_2P^*$ to HV^{2+} (0.56 eV).

becomes 280 times larger than the corresponding value of a similar porphyrin SAM cell on a gold electrode due to the suppression of undesirable EN quenching of $^1P^*$ by the electrode. Photocurrent generation was further enhanced using SAMs of porphyrin−fullerene linked molecules on ITO electrodes, as compared to the corresponding porphyrin SAM systems. The photocurrent generation mechanism was confirmed successfully by fluorescence lifetime measurements together with time-resolved transient absorption studies on the ITO systems. The surface structures of porphyrin−fullerene SAMs on ITO have been revealed in molecular resolution for the first time. These results clearly demonstrate that utilization of fullerenes as electron acceptors linked with porphyrin chromophores on ITO electrodes is highly promising for the construction of artificial photosynthetic systems.

Experimental Section

General. Melting points were recorded on a Yanagimoto micromelting apparatus and are not corrected. ^1H NMR spectra were measured on a JEOL EX-270. Fast atom bombardment (FAB) mass spectra (MS) were measured on JEOL JMS-DX303HF. UV−visible spectra were obtained on a Shimadzu UV-3100 spectrometer. AFM measurements were performed in air or in water with tapping mode using NanoScope IIIa (Veeco metrology group/ Digital Instruments). The roughness factor of the ITO surface ($R = 1.3$) was determined by the AFM measurements. All solvents and chemicals were of reagent grade quality, purchased commercially, and used without further purification unless otherwise noted. Tetrabutylammonium hexafluorophosphate used as a supporting electrolyte for the electrochemical measurements was obtained from Tokyo Kasei Organic Chemicals and recrystallized from methanol. Dry toluene and dry methylene chloride were heated at reflux and distilled from CaH_2. Thin-layer chromatography and flash column chromatography were performed with Alt. 5554 DC-Alufolien Kieselgel 60 F_{254} (Merck) and Fujisilica BW300, respectively.

Materials. ITO electrodes (190−200 nm ITO on transparent glass slides) were commercially available from Evers, Inc. (Japan). The roughness factor ($R = 1.3$) was estimated by AFM measurement with tapping mode. Gold electrodes for electrochemical and photoelectrochemical measurements ($R = 1.1$) were prepared by a vacuum deposition technique with titanium (5−10 nm) and gold (20−100 nm) in a sequence onto an Si(100) wafer, whereas, for UV−visible absorption measurements, gold (20 nm) was evaporated onto a transparent glass slide ($R = 1.5$).[8c] The roughness factor was estimated by iodine chemisorption on an Au(111) surface.

Cyclic Voltammetry Measurements. All electrochemical studies were performed on a Bioanalytical Systems, Inc. CV-50W voltammetric analyzer using a standard three-electrode cell with a modified ITO or Au working electrode (electrode area, 0.48 cm^2), a platinum wire counter electrode, and an Ag/AgCl (sat. KCl) reference electrode in CH_2Cl_2 containing a 0.2 M n-Bu$_4$NPF$_6$ electrolyte with a sweep rate of 0.10 V s^{-1}. The adsorbed amounts of compounds were determined from the charge of the anodic peak of the porphyrin first oxidation.

Photoelectrochemical Measurements. Photoelectrochemical measurements were performed in a one-compartment Pyrex UV cell (5 mL). The cell was illuminated with monochromatic excitation light through interference filters (MIF-S, Vacuum Optics Corporation of Japan) by a 180 W UV lamp (Sumida LS-140V) or monochromator (Ritsu MC-10N) by a 500 W xenon lamp (Ushio XB-50101AA-A) on a SAM of 0.48 cm^2. The photocurrent was measured in a three-electrode arrangement (Bioanalytical Systems, Inc. CV-50W), a modified ITO or Au working electrode (electrode area, 0.48 cm^2), a platinum wire counter electrode (the distance between electrodes was 0.3 mm), and an Ag/AgCl (sat. KCl) reference electrode. The light intensity was monitored by an optical power meter (Anritsu ML9002A) and corrected. Quantum

yields were calculated based on the number of photons absorbed by the chromophore on the gold electrodes at each wavelength using the input power, the photocurrent density, and the absorbance determined from the absorption spectrum on the ITO or gold electrode.

Fluorescence Lifetime Measurements. Fluorescence decays were measured by using a femtosecond pulse laser excitation and a single-photon counting system for fluorescence decay measurements.[45] The laser system was a mode-locked Ti:Sa laser (Coherent, Mira 900) pumped by an argon ion laser (Coherent, Innova 300). The repetition rate of a laser pulse was 2.9 MHz with a pulse picker (Coherent, model 9200). The third harmonic generated by an ultrafast harmonic system (Inrad, model 5−050) was used as an excitation source. The excitation wavelength was set at 425 or 435 nm, and temporal profiles of fluorescence decay and rise were recorded by using a microchannel plate photomultiplier (Hamamatsu R3809U). Full width at half-maximum (fwhm) of the instrument response function was 36 ps where the time interval of the multichannel analyzer (CANBERRA, model 3501) was 2.6 ps in the channel number. Criteria for the best fit were the values of χ^2 and the Dubrin−Watson parameters, obtained by nonlinear regression.

Femtosecond Transient Absorption Measurements. The dual-beam femtosecond time-resolved transient absorption spectrometer consisted of a self-mode-locked femtosecond Ti:sapphire laser (Coherent, MIRA), a Ti:sapphire regenerative amplifier (Clark MXR, CPA-1000) pumped by a Q-switched Nd:YAG laser (ORC-1000), a pulse stretcher/compressor, an OPG-OPA system, and an optical detection system.[46] A femtosecond Ti:sapphire oscillator pumped by a cw Nd:YVO4 laser (Coherent, Verdi) produced a train of 60 fs mode-locked pulses with an averaged power of 600 mW at 800 nm. The seed pulses from the oscillator were stretched ($\sim$250 ps) and sent to a Ti:sapphire regenerative amplifier pumped by a Q-switched Nd:YAG laser operating at 1 kHz. The femtosecond seed pulses and Nd:YAG laser pulses were synchronized by adjusting an electronic delay between the Ti:sapphire oscillator and Nd:YAG laser. Then, the amplified pulse train inside the Ti:sapphire regenerative amplifier cavity was cavity dumped by using the Q-switching technique, and about 30 000-fold amplification at 1 kHz was obtained. After recompression, the amplified pulses were color tuned by optical parametric generation and the optical parametric amplification (OPG-OPA) technique. The resulting laser pulses had a pulse width of $\sim$150 fs and an average power of 5−30 mW at 1 kHz repetition rate in the range 550−700 nm. The pump beam was focused to a 1 mm diameter spot, and laser fluence was adjusted less than $\sim$1.0 mJ cm^{-2} by using a variable neutral-density filter. The fundamental beam remaining in the OPG-OPA system was focused onto a flowing water cell to generate a white light continuum, which was again split into two parts. One part of the white light continuum was overlapped with the pump beam at the sample to probe the transient, while the other part of the beam was passed through the sample without overlapping the pump beam. The time delay between pump and probe beams was controlled by making the pump beam travel along a variable optical delay. The white continuum beams after sample were sent to a 15 cm focal length spectrograph (Acton Research) through each optical fiber and then detected by the dual 512 channel photodiode arrays (Princeton Instruments). The intensity of the white light of each 512 channel photodiode array was processed to calculate the absorption difference spectrum at the desired time delay between pump and probe pulses. To obtain the time-resolved transient absorption difference signal at the specific wavelength, the monitoring wavelength was selected by using an interference filter. By chopping the pump pulses at 43 Hz, we were able to detect the modulated probe pulses as well as the reference pulses by two separate photodiodes. The output current was amplified with a homemade fast preamplifier, and then the resultant

(45) (a) Boens, N.; Tamai, N.; Yamazaki, I.; Yamazaki, T. *Photochem. Photobiol.* **1990**, *52*, 911. (b) Nishimura, Y.; Yasuda, A.; Speiser, S.; Yamazaki, I. *Chem. Phys. Lett.* **2000**, *323*, 117.
(46) Cho, H. S.; Song, N. W.; Kim, Y. H.; Jeoung, S. C.; Hahn, S.; Kim, D.; Kim, S. K.; Yoshida, N.; Osuka, A. *J. Phys. Chem. A* **2000**, *104*, 3287.

voltage signals of the probe pulses were gated and processed by a boxcar averager. The resultant modulated signal was measured by a lock-in amplifier and then fed into a personal computer for further signal processing.

Supporting Information Available: The synthesis and characterization of compounds **1**−**8** and **H₂P-ref** and experimental details are described in the Supporting Information (S1−S11). This material is available free of charge via the Internet at http://pubs.acs.org.

JA034913F